

# Physiological and thylakoid ultrastructural changes in cyanobacteria in response to toxic manganese concentrations

Karen Ann Ferreira Moura<sup>1</sup> · Claudineia Lizieri<sup>1</sup> · Maione Wittig Franco<sup>1</sup> · Marcelo Gomes Marçal Vieira Vaz<sup>2,3</sup> · Wagner L. Araújo<sup>2,3</sup> · Peter Convey<sup>4</sup> · Francisco Antônio Rodrigues Barbosa<sup>1</sup>

Accepted: 12 August 2019 / Published online: 30 August 2019  
© Springer Science+Business Media, LLC, part of Springer Nature 2019

## Abstract

In this study, two cyanobacterial strains (morphologically identified as *Microcystis novacekii* BA005 and *Nostoc paludosum* BA033) were exposed to different Mn concentrations: 7.0, 10.5, 15.7, 23.6 and 35.4 mg L<sup>-1</sup> for BA005; and 15.0, 22.5, 33.7, 50.6, and 76.0 mg L<sup>-1</sup> for BA033. Manganese toxicity was assessed by growth rate inhibition (EC<sub>50</sub>), chlorophyll *a* content, quantification of Mn accumulation in biomass and monitoring morphological and ultrastructural effects. The Mn EC<sub>50</sub> values were 16 mg L<sup>-1</sup> for BA005 and 39 mg L<sup>-1</sup> for BA033, respectively. Reduction of chlorophyll *a* contents and ultrastructural changes were observed in cells exposed to Mn concentrations greater than 23.6 and 33.7 mg L<sup>-1</sup> for BA005 and BA033. Damage to intrathylakoid spaces, increased amounts of polyphosphate granules and an increased number of carboxysomes were observed in both strains. In the context of the potential application of these strains in bioremediation approaches, BA005 was able to remove Mn almost completely from aqueous medium after 96 h exposure to an initial concentration of 10.5 mg L<sup>-1</sup>, and BA033 was capable of removing 38% when exposed to initial Mn concentration of 22.5 mg L<sup>-1</sup>. Our data shed light on how these cyanobacterial strains respond to Mn stress, as well as supporting their utility as organisms for monitoring Mn toxicity in industrial wastes and potential bioremediation application.

**Keywords** Manganese · Toxicity · Cyanobacteria · Ultrastructure · Bioremoval

## Introduction

Manganese (Mn) is an essential micronutrient that may become toxic if present at high concentration. In humans, exposure to high levels of Mn results in neurological and neuropsychiatric effects such as hallucination, emotional instability, weakness, as well behavior and speech

disorders, which are similar to Parkinson's disease and are named Manganism (Siqueira 1985). The majority of environmental studies available to date focus on the adverse effects of Mn on plants (Marschner 1995; Lizieri et al. 2012), which typically display symptoms including cell wall deformation, reduction of photosynthetic apparatus, stunting, burning of leaf tips and flowers, as well as shriveling of leaves (Lindon et al. 2004; Reichman 2002; Lizieri et al. 2012; Carrasco-Gil et al. 2015). Nevertheless, little is currently known concerning the effects of Mn on aquatic communities, and in particular on cyanobacterial populations.

To establish water quality standards and avoid chronic human contamination, the World Health Organization (WHO) recommended, until 2011, a Mn limit of 0.4 mg L<sup>-1</sup> for drinking water (Frisbie et al. 2012). In Brazil, the National Environmental Council allows 0.1 mg L<sup>-1</sup> Mn as the maximum permissible limit (MPL) for water supply for human consumption and 1.0 mg L<sup>-1</sup> in effluent discharge (Brazil 2005). Higher values are frequently found in water resources in several countries, including Brazil, due mainly to natural Mn deposits in rock (Roy 1997). Natural sources

✉ Maione Wittig Franco  
maionewf@hotmail.com

<sup>1</sup> Laboratório de Limnologia, Ecotoxicologia e Ecologia Aquática, Instituto de Ciências Biológicas, B. I3, 163, Universidade Federal de Minas Gerais, Avenida Antonio Carlos, 6627, Belo Horizonte, Minas Gerais 31270-901, Brazil

<sup>2</sup> Departamento de Biologia Vegetal, Universidade Federal de Viçosa, Viçosa, Minas Gerais 36570-900, Brazil

<sup>3</sup> Max Planck Partner Group at the Departamento de Biologia Vegetal, Universidade Federal de Viçosa, Viçosa, Minas Gerais 36570-900, Brazil

<sup>4</sup> British Antarctic Survey, NERC, High Cross, Madingley Road, Cambridge CB3 0ET, UK

of Mn include direct deposition, ocean spray, forest fires and volcanic activity, while anthropogenic Mn pollution derives from municipal wastewater discharges, mineral processing (CICAD 2004), industrial activities based on outdated technologies (Duan et al. 2010) and inadequate tailing storage conditions. In November 2015, a huge environmental disaster occurred in Brazil due to the collapse of a tailings dam controlled by a local mining company at Mariana city (20° 22' 40" S; 43° 24' 58" W), in Minas Gerais state. One of the most important rivers of south-eastern Brazil (Rio Doce) was inundated with mud containing mining waste, which affected the entire river downstream and eventually reached the Atlantic coast. Water and sediment analyses from the affected areas recorded high concentrations of total Mn, iron (Fe), aluminum (Al) and other metals. In some parts of the river system Mn values around 857 mg L<sup>-1</sup> were recorded (IGAM 2017), almost four orders of magnitude greater than the Brazilian MPL for drinking water.

Given this scenario, the search for clean technologies for water decontamination has stimulated research into the application of microorganisms for metal immobilization (Farag et al. 1998; Ji et al. 2012). In the process of the remineralization of nutrients, some microscopic phytoplankton are able to bioaccumulate toxic organic or inorganic compounds (Bonaventura and Johnson 1997; Vidali 2001; Franco et al. 2015). However, the knowledge of the bioaccumulation potential of Mn on cyanobacteria and microalgae is limited to few species and its toxic effects are currently not well understood (Mohamed 2001; Dohnalkova et al. 2006; Brandenburg et al. 2017).

Among phytoplankton groups, some cyanobacteria have been highlighted as excellent models to evaluate and monitor environmental pollution (Campos et al. 2013). Over evolutionary time, these organisms have developed diverse strategies enabling toleration of toxic elements in the surrounding medium (Perales-Vela et al. 2006). Furthermore, some cyanobacterial strains can combine an autotrophic mode of growth with mixotrophy, which enables their growth using various organic carbon sources (Chojnacka and Noworyta 2004). The combination of cellular and structural adaptations allows their survival under a wide range of environmental conditions (Komárek and Anagnostidis 1998, 2013). Due to their biochemical, physiological and anatomical characteristics, cyanobacteria are used in various biotechnological processes, including bioremediation (Pokrovsky et al. 2008; Pereira et al. 2011; Kumar et al. 2012) and the assessment of element toxicity, including As (Pandey et al. 2012; Franco et al. 2015), Pb (Arunakumara and Xuecheng 2009) and other toxic elements (Hudek et al. 2012).

In this study we investigated the effects of exposure to varying concentrations of Mn on the physiological and

ultrastructural characteristics, growth rate, and bioremediation capacity of a coccoid and a filamentous-heterocytous cyanobacterial strain. The data obtained shed light on cyanobacterial responses to Mn exposure and the bioremediation potential of these two strains, as well as enhancing understanding of Mn toxicity on aquatic organisms.

## Material and methods

### Cyanobacterial identification

Two morphologically distinct cyanobacteria, a unicellular strain (BA005) and a filamentous heterocytous strain (BA033) were selected. The strain BA005 was isolated from water samples collected at the Dom Helvécio lake, Parque Estadual do Rio Doce (19° 46' 55" S; 42° 35' 28" W) and the strain BA033 was obtained from a stream water sample obtained downstream of a gold processing plant in the municipality of Nova Lima (19° 58' 74.8" S; 43° 49' 25.9" W), both sampling sites located in Minas Gerais state, Brazil. Cultures of BA005 were maintained in ASM-1 medium (Gorham et al. 1964) and those of BA033 in BG-11<sub>0</sub> (Allen and Stanier 1968), the media being chosen after initial trials (data not shown). Both cultures were maintained in a growth chamber at 21.0 ± 1.0 °C, under constant illumination from white cold fluorescent lamps, with intensity of 110 μmol photons m<sup>-2</sup> s<sup>-1</sup> (OSBRAM, lumilux-cool, 16 W, Brazil) at the Microalgae and Cyanobacteria Culture Collection of the Laboratory of Limnology, Ecotoxicology and Aquatic Ecology of the Institute of Biological Sciences, Universidade Federal de Minas Gerais, Brazil. For taxonomic identification, morphological diacritical traits were examined under an optical light microscope (Zeiss AxioCam ICc1) and molecular analyses were carried out. For molecular analysis, the total genomic DNA was extracted from 2–3 mL of 14 days-old cultures, applying the UltraClean<sup>®</sup> Microbial DNA Isolation Kit (MoBio, Carlsbad, CA). Partial 16S rRNA gene sequence was amplified by PCR, using the primers 27F1 (Neilan et al. 1997) and 23S30R (Taton et al. 2003) as described previously (Genuário et al. 2013). The PCR products were cloned in a pGEM-T Easy Vector System (Promega, Madison, WI, USA) following the manufacturer's instructions, and competent *Escherichia coli* DH5α cells were then submitted to transformation. The plasmids containing the cyanobacterial 16S-23S fragments were purified using the UltraClean<sup>®</sup> Standard Mini Plasmid Prep Kit (MoBio, Carlsbad, CA), and were then sequenced following Genuário et al. (2013) and Vaz et al. (2015). Two independent phylogenetic reconstructions were carried out, the first for 16S rRNA sequences of unicellular morphotypes, and the second for sequences retrieved from filamentous heterocytous

morphotypes. The 16S gene fragment sequences obtained in this study and related ones obtained from GenBank were aligned using CLUSTAL W and trimmed. For the unicellular phylogenetic tree, a total of 62 16S rRNA sequences were used, generating a matrix of 1369-bp length. For the nostocacean (filamentous heterocytous) phylogenetic tree, 105 16S rRNA sequences were used in a matrix with 1442-bp length. In both cases the phylogeny was inferred based on the Maximum Likelihood (ML) method. The Kimura 2-parameter model with gamma distributed with invariant sites (K2 + G + I) was selected as the best-fitting model, applying the model-testing function in MEGA version 5 (Tamura et al. 2011). The robustness of the phylogenetic trees was estimated by bootstrap analysis using 1000 replications.

The new nucleotide sequences have been deposited in the NCBI GenBank database under the accession numbers KX423683 and KX423684, for *Microcystis novacekii* BA005 and *Nostoc paludosum* BA033, respectively.

### Acute toxicity test

Manganese toxicity tests were performed following the recommended methodology of OECD 201 (2011). Replicates consisted of cyanobacterial cultures prepared in 250 mL Erlenmeyer flasks containing 150 mL of culture medium (pH = 7.0 ± 0.2). Initial cell concentration was 10<sup>5</sup> cells mL<sup>-1</sup>. The experiment was conducted under the growth conditions described above. Once exponential growth phase was reached, cultures were exposed to increasing concentrations of Mn. A stock solution of 15 g L<sup>-1</sup> was prepared from MnCl<sub>2</sub>·4H<sub>2</sub>O and was added to the cultures, to give the following Mn concentrations: 7.0, 10.5, 15.7, 23.6, and 35.4 mg L<sup>-1</sup> for BA005 and 15.0, 22.5, 33.7, 50.6, and 76.0 mg L<sup>-1</sup> for BA033. Control groups in both experiments were the respective culture medium inoculated with cyanobacteria. The Mn concentrations used in both experiments were determined in preliminary tests (data not shown) to achieve the growth inhibition range recommended in OECD 201 protocol. Negative controls (replicates without cyanobacteria cells) were used to confirm the initial Mn concentrations in the supernatant of the cultures.

Cyanobacterial growth was monitored daily up to 96 h by measuring optical density at 680 nm (DO<sub>680nm</sub>). The equation %I = [(μ<sub>c</sub> - μ<sub>t</sub>)/μ<sub>c</sub>] × 100 was used to calculate the percentage of growth inhibition (%I), in which μ<sub>c</sub> is the average growth rate of the control group and μ<sub>t</sub> the average growth rate under Mn exposure. The equations y = 5.238x - 35.402 (r<sup>2</sup> = 0.90) for BA005 and y = 1.259x - 0.1512 (r<sup>2</sup> = 0.91) for BA033 were obtained by linear regression of the growth inhibition percentage as function of Mn concentration and used to calculate the Mn concentration that effectively reduced the growth rate by 50%. The

high r<sup>2</sup> values obtained for both strains demonstrate that the linear fit was adequate for the calculation of EC<sub>50</sub> as recommended by the OECD 201 protocol.

### Chlorophyll a content

To determine total chlorophyll a content (Chl a) after 96 h of exposure to Mn in the acute toxicity test, aliquots (10 mL) were taken from each Erlenmeyer flask and centrifuged at 5000 × g for 10 min. The supernatant was removed and 3.5 mL of methanol (90%) was added to the pellet, which was then vigorously stirred in a manual shaker (Vortex) for 30 s and left for 25 min in the dark at room temperature. The absorbance (UV/Visible Hitachi U-200) was measured at 665 nm and the Chl a was determined by the equation: Chlorophyll a (mg L<sup>-1</sup>) = α × Absorbance 665 nm, where α is the absorption coefficient for Chl a extracted with methanol (α = 12.7) (Meeks and Castenholz 1971; Modified by Fiore et al. 2000).

### Mn determination in biomass

After 96 h of exposure to Mn in the acute toxicity test, 30 mL aliquots of each replicate were centrifuged (20 min, 1569 × g) and the biomass obtained was divided in two subsamples: one washed with Mes-EDTA buffer to remove the Mn atoms attached to cells by physicochemical process (biosorbed) and the other was washed with ultrapure water (Milli-Q) to quantify the total Mn bioaccumulated in cells (as a result of physicochemical and biological processes). Washing consisted of adding Mes-EDTA buffer (pH = 5) or ultrapure water to the pellet, vortexing the sample, and centrifuging (20 min, 1569 × g); this procedure was repeated three times. The biomass samples were dried at room temperature, in a desiccator until constant mass and were mineralized by adding 3 mL of concentrated HNO<sub>3</sub> (96%) and 1 mL of H<sub>2</sub>O<sub>2</sub> (30%) in Teflon tubes (Truus et al. 2007). Samples were heated in a microwave accelerated reaction system (ETHOS One model, Milestone Microwave Systems, Shelton, USA) for 30 min at 200 °C and pressure of 45 bar. The final volume was adjusted to 25 mL with ultrapure water and kept under refrigeration (7 °C) until analysis. All Mn determinations were performed by inductively coupled plasma optical emission spectrometry (Perkin Elmer Optima 4300 DV). The values of Mn in biomass were expressed in mg Mn g<sup>-1</sup> of biomass.

### Mn determination in solution

After 2 and 96 h of Mn addition in the acute toxicity test, subsamples of 10 mL of all replicates were collected and centrifuged (1569 × g, 10 min, 25 °C) and the supernatant obtained was filtered through a glass fiber membrane

(1.2  $\mu\text{m}$ ), acidified with concentrated  $\text{HNO}_3$  (96%) and kept under refrigeration until analysis. Subsamples of the negative control were collected after 2 h of the Mn addition, acidified with concentrated  $\text{HNO}_3$  (96%) and kept under refrigeration until analysis in ICP-OES. The Mn fraction removed from the supernatant was expressed as a percentage of the Mn concentration measured in the negative control.

### Ultrastructural effects of Mn exposure

For transmission electron microscopy (TEM) analysis, aliquots (10 mL) from all treatments in the Mn acute toxicity test (96 h) were fixed in glutaraldehyde (2.5%) in phosphate buffer (0.05 M, pH 7.0) for 24 h and washed three times in phosphate buffer (0.1 M). The fragments were post-fixed in osmium tetroxide (1%) prepared in the same buffer and left for 4 h. They were then dehydrated in an ascending ethanol series before embedding in Spurr's resin (Spurr 1969) and the blocks were polymerized at 650  $^\circ\text{C}$  for 20 h. Ultra-thin sections were obtained with the aid of an ultramicrotome (Sorvall Model MT-2). Post-staining took place in uranyl acetate and lead citrate (Reynolds 1963). The samples were then examined in a transmission electron microscope (FEI, Tecnai G2 Spirit TWIN, 120 kV) in the Center of Microscopy of the Universidade Federal de Minas Gerais.

### Statistical analyses

Cyanobacterial growth was analyzed using two-way analysis of variance (ANOVA) with respect to the two factors, namely Mn concentration and time, and the means were compared pairwise using Tukey's post hoc test ( $p < 0.05$ ). The average Chl *a* content was compared between groups ( $n = 3$ ) using ANOVA and the means compared pairwise using Tukey's post hoc test ( $p < 0.05$ ). The accumulated Mn

in the biomass as a function of the concentration of Mn in the medium was analyzed using linear regression or a second order polynomial adjustment, according to the best fit of the data for each species of cyanobacteria.

## Results

### Cyanobacterial identification

After morphological inspection of diacritical traits, the unicellular strain BA005 was assigned to the morphospecies *Microcystis novacekii* (Komárek) Compère 1974:19, which is typified by free-floating colonies with individual cells forming thick aggregates in the center of the colony and with very few isolated cells in the periphery; after division the cells are spherical or hemispherical (Komárek and Anagnostidis 1998, 2013). The filamentous heterocytous strain BA033 was morphologically identified as *Nostoc paludosum* Kützing ex Bornet et Flahault 1886:191, and has aggregated filaments, slightly straight, unbranched, with intercalary and terminal heterocytes, production of mucilage and sometimes forming colonies. The trichomes are isopolar, uniseriate and usually constricted (Komárek and Anagnostidis 2013).

Partial 16S rRNA gene sequences were obtained for both strains: 1354 bp for BA005 and 1412 bp for BA033. Analyses applying the BLAST tool (NCBI) showed identities greater than 99.1% and ranging from 96.8% to 99%, respectively, with sequences retrieved from *Microcystis* and *Nostoc* morphotypes (Table 1).

In the phylogenetic reconstruction based on the 16S rRNA partial sequences from unicellular strains (Fig. 1) the sequence obtained from *M. novacekii* BA005 grouped together with other sequences from *Microcystis* spp. morphotypes and also with sequences from uncultured

**Table 1** Sequence identity (%) of 16S rRNA gene fragments among UFMG strains and other cyanobacterial strains available in GenBank

Code	Length (bp)	Closest match (accession number)	C <sup>b</sup> (%)	I <sup>c</sup> (%)
<i>Microcystis</i> sp.	1354	<i>Microcystis</i> sp. 0901-4C (AB936780) <sup>a</sup>	100	99.2
		<i>Microcystis aeruginosa</i> NIES-2549 (CP011304)	100	99.1
		<i>Microcystis</i> sp. 130 (AJ133170)	100	99.1
		<i>Microcystis ichthyoblabe</i> VN325 (AB666073)	99	99.2
		<i>Microcystis aeruginosa</i> OBB35S02 (AJ635430)	100	99.1
		<i>Nostoc</i> sp.	1412	<i>Nostoc</i> sp. TH1S01 (AM711547)
<i>Nostoc</i> sp.	1412	<i>Nostoc</i> sp. SAG 2306 (GQ287649)	100	98.2
		<i>Nostoc</i> sp. PCC9426 (AM711538)	100	97.8
		<i>Trichormus azollae</i> Kom BAI/1983 (AJ630454)	100	97.3
		<i>Nostoc piscinale</i> CENA21 (AY218832)	100	96.8

<sup>a</sup>Published sequences of culturable strains

<sup>b</sup>Coverage

<sup>c</sup>Identity

**Fig. 1** Maximum likelihood phylogenetic tree based on 16S rRNA gene sequences of unicellular strains. The sequence from the novel strain, *Microcystis novacekii* BA005, is shown in bold with a black circle. A bootstrap test involving 1000 resamplings was performed and bootstrap values greater than 50% are given in the relevant nodes



organisms in a robust cluster (100% bootstrap value). In the phylogeny from nostocacean strains (Fig. 2) the sequence retrieved from BA033 was placed in a cluster with other sequences of *Nostoc*, *Anabaenopsis* and *Trichormus* morphotypes (89% bootstrap values—cluster G-I). As an internal group (Fig. 2, subcluster G-Ia), with 50% bootstrap value, the sequence of BA033 grouped with sequences which shared the highest identity values (Table 1). The cluster G-I is not related to the true group of the genus *Nostoc* (*Nostoc* spp. *sensu stricto*) and is also separated from the recently described new genera *Desmonostoc*, *Mojavia* and *Halotia*, reinforcing the polyphyletic status of the genus *Nostoc*.

### Acute toxicity test

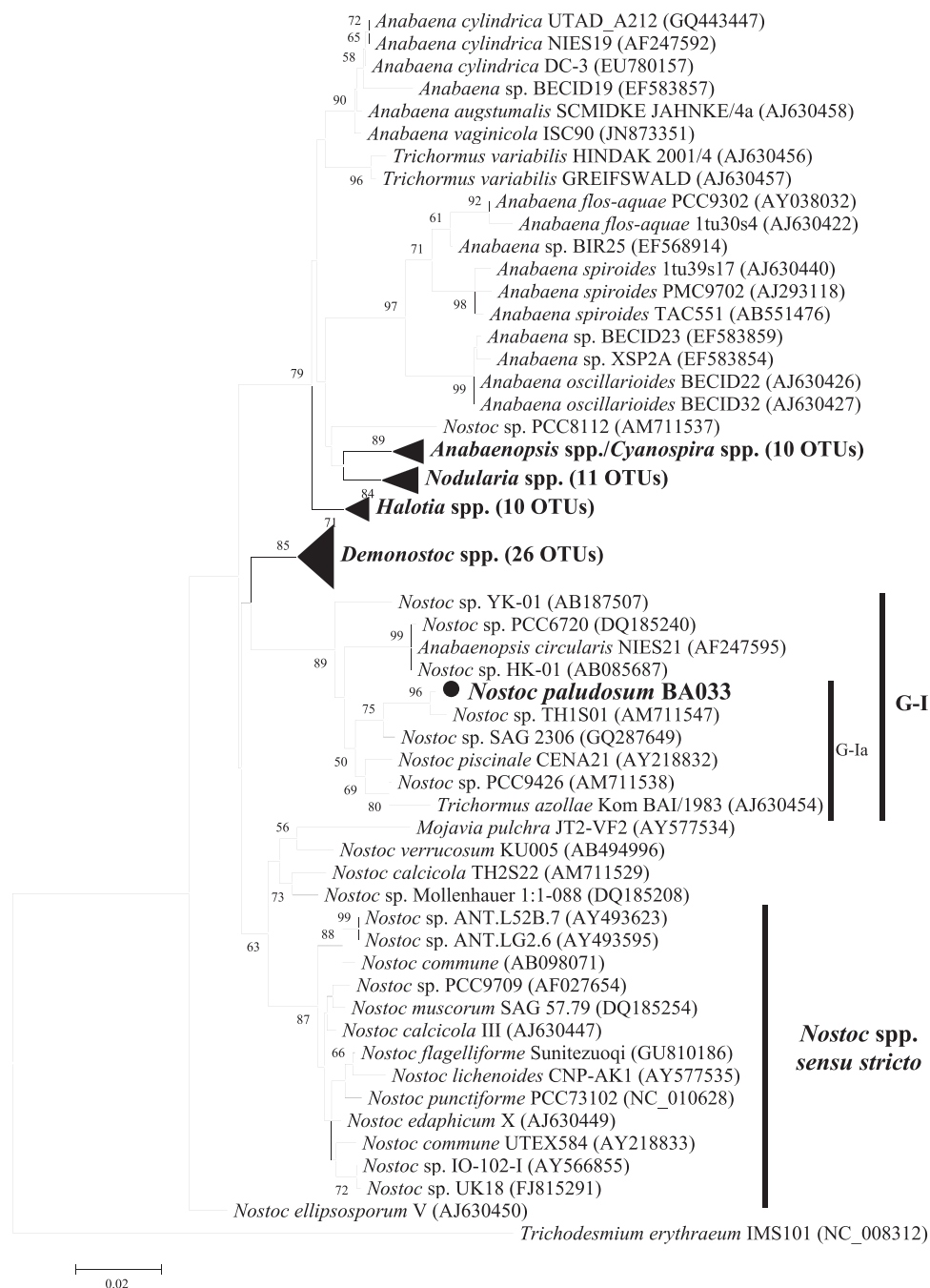
Manganese affected cyanobacterial growth as a function of concentration and exposure time. The EC<sub>50</sub> value obtained for BA005 was 16 mg L<sup>-1</sup> (with a 95% confidence interval of 11 to 21 mg L<sup>-1</sup>), and for BA033 was 39 mg L<sup>-1</sup> (with a

95% confidence interval of 23 to 55 mg L<sup>-1</sup>) (Fig. 3). When exposed to 7.0 mg L<sup>-1</sup> Mn, no effect on growth of BA005 (Fig. 4a) was observed after 96 h ( $p = 0.34$ ). However, at 35.4 mg Mn L<sup>-1</sup>, negative effects were detected after 24 h ( $p < 0.01$ ), while after 48 h significant growth inhibition was observed at 23.6 and 35.4 mg Mn L<sup>-1</sup> ( $p < 0.01$ ). After 96 h growth inhibition was significant at concentrations of 10.5, 15.7, 23.6, and 35.4 mg Mn L<sup>-1</sup> ( $p < 0.01$ ). Growth inhibition of BA033 (Fig. 4b) was initially detected after 48 h of exposure to 50.6 and 76.0 mg Mn L<sup>-1</sup> ( $p < 0.01$ ). After 96 h negative effects on growth were apparent at all Mn concentrations used ( $p < 0.05$ ).

### Chlorophyll *a* content

After 96 h of Mn exposure, the Chl *a* content increased in cells of BA005 exposed to 15.7 mg L<sup>-1</sup> ( $p < 0.01$ ) and showed a significant decrease at concentrations of 23.6 and 35.4 mg L<sup>-1</sup> ( $p < 0.01$ ) (Fig. 5a). In contrast, in tests with

**Fig. 2** Maximum likelihood phylogenetic tree based on 16S rRNA gene sequences of Nostocacean strains. The sequence from the novel strain, *Nostoc paludosum* BA033, is shown in bold with a black circle. A bootstrap test involving 1000 resamplings was performed and bootstrap values greater than 50% are given in the relevant nodes



BA033 a gradual decrease in Chl *a* content (Fig. 5b) was observed with increasing Mn concentration ( $p < 0.01$ ).

### Mn bioaccumulation in biomass

In both strains the quantification of Mn in the biomass washed with MES-EDTA was below the detection limit ( $0.005 \text{ mg g}^{-1}$ ; data not shown). On the other hand, for both strains the amount of Mn bioaccumulated in the biomass washed with ultrapure water increased with higher Mn concentration in the culture medium (Fig. 6).

For the strain BA005, at the lower Mn concentrations ( $7.0$  and  $10.5 \text{ mg L}^{-1}$ ) biosorption values were  $0.026$  and  $0.059 \text{ mg g}^{-1}$  (mg of Mn per g of biomass), at the intermediate Mn concentration ( $15.7 \text{ mg L}^{-1}$ ), the biosorption was  $0.11 \text{ mg g}^{-1}$ , and at the highest Mn concentrations ( $23.6$  and  $35.4 \text{ mg L}^{-1}$ ) the biosorption values were similar in both treatments ( $0.167$  and  $0.175 \text{ mg g}^{-1}$ ), suggesting a possible saturation effect on binding sites at Mn concentrations of  $23.6 \text{ mg L}^{-1}$  and above. The strain BA033 showed increased biosorption values with increasing Mn concentration in the culture medium:  $0.025$

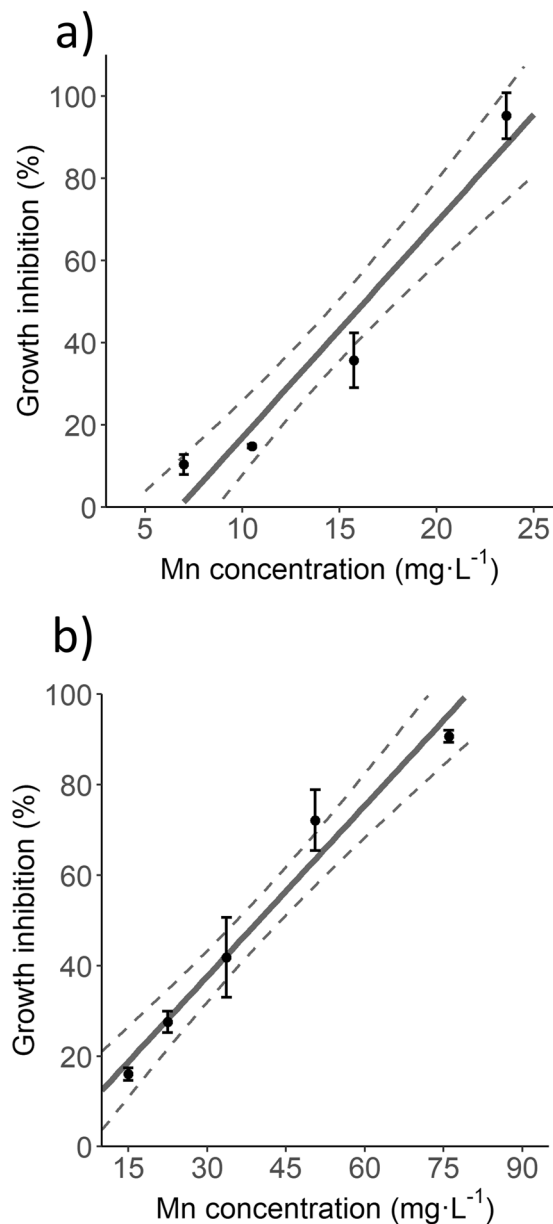


**Fig. 3** Percentage growth inhibition after 96 h of Mn exposure. **a** *Microcystis novacekii* BA005,  $y = 5.238x - 35.402$  ( $r^2 = 0.90$ ); **b** *Nostoc paludosum* BA033,  $y = 1.259x - 0.1512$  ( $r^2 = 0.91$ ). Points are average  $\pm$  SE

and  $0.041 \text{ mg g}^{-1}$  in the lower Mn concentrations ( $15.0$  and  $22.5 \text{ mg L}^{-1}$ , respectively),  $0.061 \text{ mg g}^{-1}$  at the intermediate Mn concentration ( $33.7 \text{ mg L}^{-1}$ ), and  $0.079$  and  $0.139 \text{ mg g}^{-1}$  at Mn concentrations of  $50.6$  and  $76.0 \text{ mg L}^{-1}$ , respectively.

### Mn concentration in solution

Considering the Mn concentration in solution (Table 2), a decrease in Mn content was observed in the first 2 h of exposure in both cyanobacterial strains. In addition, the

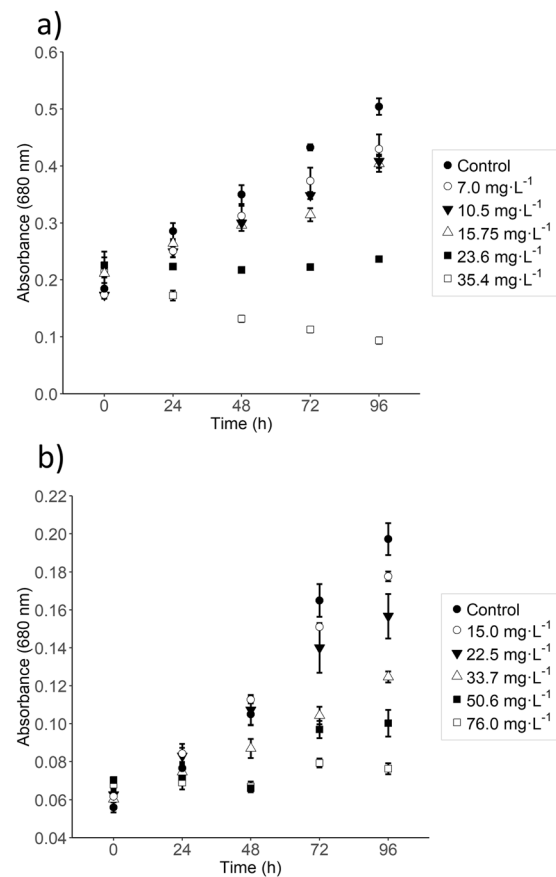


**Fig. 4** Growth of *Microcystis novacekii* BA005 (**a**) and *Nostoc paludosum* BA033 (**b**) during 96 h exposure to different Mn concentrations. Points are average  $\pm$  SE

percentage of Mn removed was greater with longer exposure time (96 h), especially using strain BA005 when Mn concentration in solution was reduced by more than 90% from starting concentrations of  $7.0$  to  $15.7 \text{ mg L}^{-1}$ . However, the percentage of Mn removed decreased to values of 31% and 14%, respectively, at the highest Mn concentrations tested in both species. The negative control (culture medium without cyanobacteria) indicated variations of less than 10% from the expected initial Mn concentration in both strains, confirming accuracy in the experimental procedures (Table 2).

### Ultrastructural effects of Mn exposure

Ultrastructural analyses indicated that morphological changes were apparent in both strains after exposure to Mn concentrations above  $15.0 \text{ mg L}^{-1}$ . These included swelling of intrathylakoid spaces, presence of increased numbers of carboxysomes and polyphosphate granules, and increased periplasmic space (Fig. 7). All these effects became more intense with increasing Mn concentration.

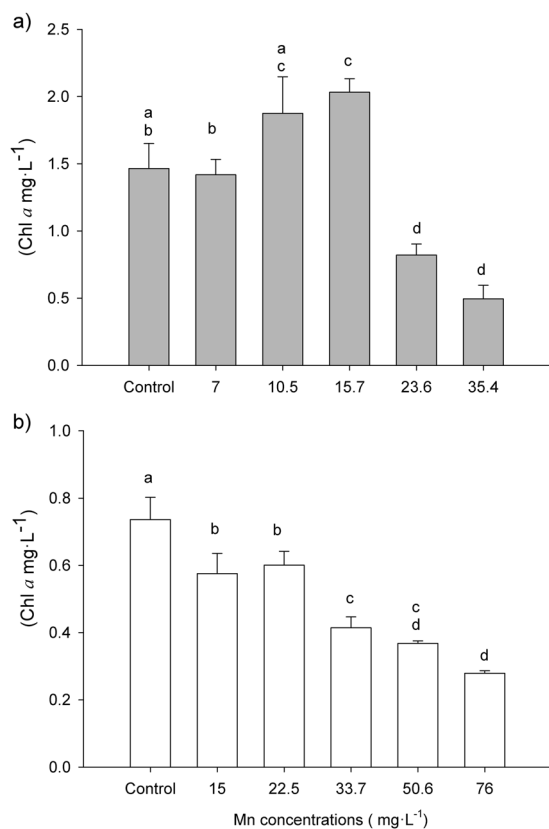


**Fig. 5** Chlorophyll *a* content in cyanobacteria biomass after 96 h exposure to different Mn concentrations. **a** *Microcystis novacekii* BA005; **b** *Nostoc paludosum* BA033. Bars indicate SD, different letters indicate significant differences between groups

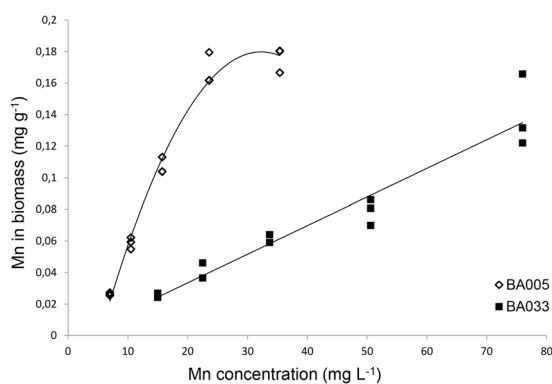


**Fig. 6** Manganese (Mn) biosorption by cyanobacterial biomass at different concentrations. White squares: *Microcystis novacekii* BA005 ( $y = -0.0002x^2 + 0.016x - 0.0779$ ,  $r^2 = 0.98$ ). Dark squares: *Nostoc paludosum* BA033 ( $y = 0.0018x - 0.0028$ ,  $r^2 = 0.92$ )

## Discussion

### Cyanobacterial identification

The toxic effects following exposure to particular elements are likely to be influenced by the microbial species

examined. Therefore, reliable identification is required in order to perform toxicological tests. Two distinct cyanobacterial strains were used in the current study, one being unicellular and the other filamentous heterocytous. Molecular and morphological analyses of the unicellular strain (BA005) confirmed that it is a representative of *Microcystis* (Fig. 1). Although the genus *Microcystis* is monophyletic, species delimitation within the genus remains problematic (Komárek et al. 2014; Genuário et al. 2016). Representatives of *Microcystis* are exclusively planktonic, and this is one of the most important bloom-forming genera in freshwater environments. Detailed studies have been made of the ecology and toxicological responses of members of this genus (Komárek 2016; Genuário et al. 2016).

Members of the genus *Nostoc* are typified by having uniseriate, isopolar and non-branched filaments, and its vegetative cells can differentiate into akinetes (formed apoheterocytically), heterocytes (terminal and intercalary) and hormogonia (Komárek and Anagnostidis 1989). Other traits including production of mucilaginous colonies and possession of specific life cycles are common to members of this genus (Mateo et al. 2011; Hrouzek et al. 2013; Genuário et al. 2015). However, these morphological traits are insufficient for generic delimitation, and the genetic diversity of apparent ‘*Nostoc*’ strains is more complex than their morphological differentiation. Phylogenetic analysis of 16S rRNA sequence data obtained from *Nostoc* morphotypes have revealed that many genotypes fall outside the *Nostoc* spp. *sensu stricto* cluster (Hrouzek et al. 2013; Papaefthimiou et al. 2008; Genuário et al. 2015), as was observed in the current study for the strain BA033 (Fig. 2). As a consequence, this genus has been under constant revision, culminating with the erection of novel genera, which are morphologically similar to *Nostoc* morphotypes but form different evolutionary lineages, e.g., *Mojavia*, *Desmonostoc* and *Halotia*. The strain BA033 could represent a new generic entity, being located in a monophyletic cluster separated from the *Nostoc* spp. *sensu stricto* cluster and also apart from other recent described *Nostoc*-related genera (Fig. 2). Furthermore, the 16S rRNA sequence obtained from strain BA033 had a low identity ( $\leq 96\%$ ) when compared with sequences of well-defined genera.

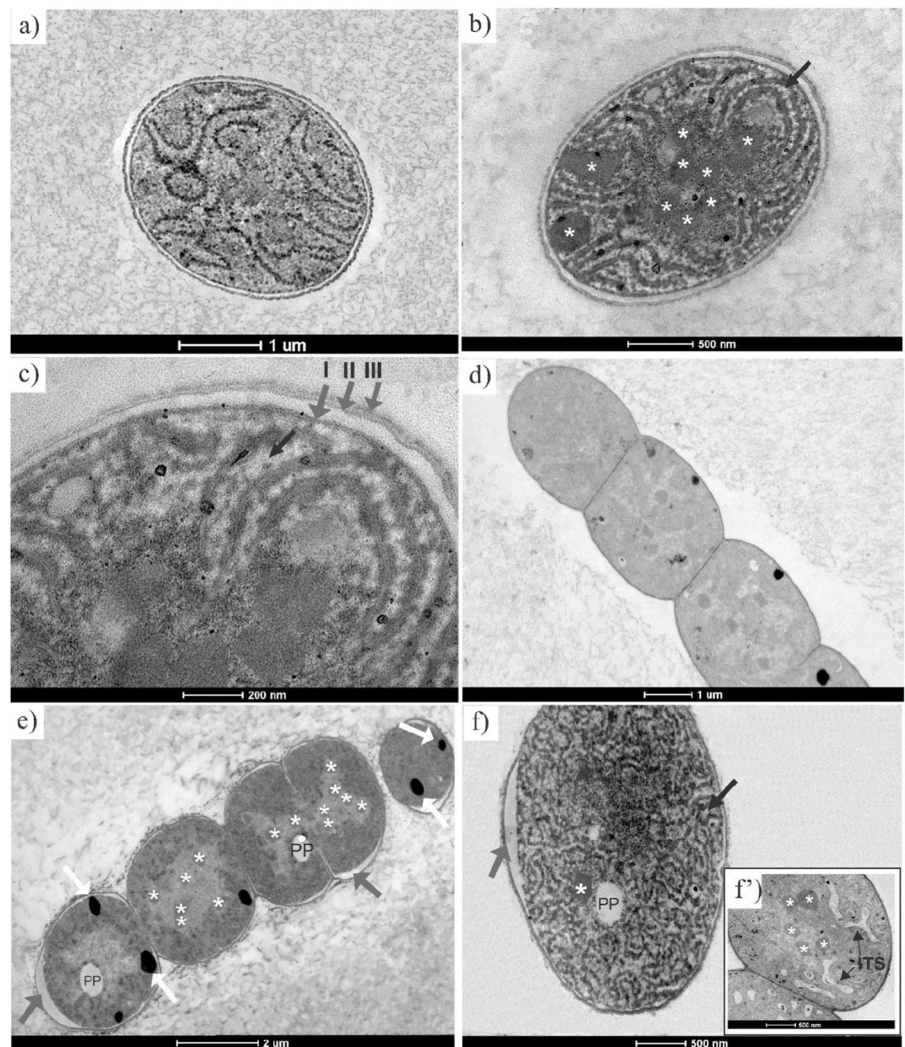
### Acute toxicity test and chlorophyll *a* content

Although both strains showed similar effects, the concentrations at which toxicity became apparent differed between them, with BA033 displaying higher tolerance to Mn ( $EC_{50} = 39 \text{ mg Mn L}^{-1}$ ) compared to BA005 ( $EC_{50} = 16 \text{ mg Mn L}^{-1}$ ) (Fig. 3). Notably, growth reductions in BA005 were observed within the first 24 h after Mn exposure, whereas BA033 only showed effects after a longer period of time (48 h) (Fig. 4). The Mn concentrations at

**Table 2** Manganese content in solution

	[Mn] (mg L <sup>-1</sup> )	Negative control (mg L <sup>-1</sup> )	Supernatant 2 h Mn exposure (mg L <sup>-1</sup> )	Removal (%) 2 h	Supernatant 96 h Mn exposure (mg L <sup>-1</sup> )	Removal (%) 96 h
<i>Microcystis novacekii</i> BA005	Control	–	0.21 ± 0.0	–	0.18 ± 0.0	–
	7.0	7.2 ± 0.0	1.57 ± 0.0	78	0.43 ± 0.3	94
	10.5	11.4 ± 0.6	2.78 ± 0.0	76	<0.06 ± 0.0	~100
	15.7	15.7 ± 0.0	6.52 ± 0.3	59	0.56 ± 0.4	96
	23.6	23.4 ± 0.2	12.96 ± 1.8	45	5.01 ± 2.2	79
	35.4	34.3 ± 0.6	24.25 ± 0.9	29	23.69 ± 0.8	31
<i>Nostoc paludosum</i> BA033	Control	–	0.28 ± 0.0	–	0.25 ± 0.0	–
	15.0	14.6 ± 0.4	13.38 ± 0.4	8	10.30 ± 0.7	29
	22.5	21.9 ± 0.7	19.62 ± 0.2	11	13.68 ± 0.8	38
	33.7	32.8 ± 1.0	29.68 ± 0.3	10	22.56 ± 0.3	31
	50.6	49.7 ± 2.0	45.23 ± 2.8	9	39.09 ± 0.2	21
	76.0	72.9 ± 3.4	69.53 ± 1.9	5	62.70 ± 0.8	14

**Fig. 7** Transmission electron microscopy micrographs of cyanobacterial strains illustrating ultrastructural changes after exposure to Mn: **a** *Microcystis novacekii* BA005–control; **b** *M. novacekii* BA005 after 96 h Mn exposure, showing carboxysomes (white asterisks) and intrathylakoid spaces (black arrow); **c** Details of the cellular shell layers after 96 h Mn exposure: the outer membrane (arrow III), peptidoglycan layer (arrow II) and plasma membrane (arrow I), and intrathylakoid spaces (black arrow); **d** *Nostoc paludosum* BA033–control; **e** *N. paludosum* BA033 showing increased periplasmic spaces (gray arrows), carboxysomes (white asterisks) and polyphosphate granules (white arrows), PP = polyphosphate granules (electron-transparent region); **f** *N. paludosum* cell showing the intrathylakoid spaces (black arrow), carboxysome (white asterisk), increased periplasmic spaces (gray arrow) and PP = polyphosphate granules (electron-transparent region); **f'** Detail of intrathylakoid spaces (ITS) and carboxysome (white asterisks)



which toxicity became apparent obtained here are consistent with previous studies. Hudek et al. (2012) found significant growth reduction in *Nostoc punctiforme* growth after 24 h of exposure to Mn concentrations higher than 750  $\mu\text{M}$

(41.2 mg L<sup>-1</sup>). The EC<sub>50</sub> values obtained for the strains analyzed here demonstrated that both are tolerant to high Mn levels, comparable to previously observed values for other cationic metals. For instance, Rangsayatorn et al.

(2002) reported an  $EC_{50}$  of  $18.35 \text{ mg L}^{-1}$  for Cd in *Spirulina (Arthrospira) platensis*.

Manganese at toxic concentrations affects cellular homeostasis by decreasing the content of chlorophyll *a*, reducing growth and significantly altering cellular ultrastructure. Cyanobacterial tolerance leading to relatively low toxicity of Mn in moderate concentrations may be related to the requirement for Mn ions in cell metabolism, given that it is an important cofactor for various enzymes and plays an essential role in the photosynthetic process (Hudek et al. 2012; Fischer et al. 2015). In contrast, the harmful effects observed at high Mn concentrations are most likely related to nutritional imbalance caused by an excess of Mn ions in solution. Manganese is often associated with iron deficiency due to competition for the site (porphyrin ring) in which iron is necessary for the synthesis of chlorophyll (Csatorday et al. 1984). Thus, it cannot be excluded that the large reductions of chlorophyll *a* content observed in this study in both tested strains may be a result of iron deficiency. The reductions in Chl *a* content were consistent with the decrease in growth rates observed in the presence of Mn, with the reduction being more prominent in BA005 compared to BA033. This is possibly due to the presence of a mucilaginous sheath around the cells of BA033, which may act as an alternative carbon source in situations of nutrient shortage. BA005 loses its characteristic mucilaginous sheath in culture conditions. Overall, our data suggest that toxic Mn concentrations affect primary productivity through interference in Chl *a* content (Fig. 5). In BA005, Chl *a* content increased following exposure to lower concentrations of Mn in concert with a small inhibition in growth (Fig. 4), consistent with expectations (OECD 201 2011). A similar effect was previously reported in *Phaseolus vulgaris* under Mn stress (Teixeira et al. 2004).

### Uptake of Mn by cyanobacterial cells

Both cyanobacterial strains investigated demonstrated capacity to remove Mn from the culture medium. BA005 showed great efficiency at initial concentrations ranging from 7 to  $15 \text{ mg Mn L}^{-1}$ , removing more than 90% of Mn in the medium (Table 2). The results obtained here corroborate a previous study which demonstrated, in mixed solution, removal of an average of 85% of the total Mn and 96% of zinc by a cyanobacterial mat allowed to grow in columns packed with glass wool (Bender et al. 1994). Similarly, Hazarika et al. (2014) demonstrated the ability of *N. muscorum* cultures in BG-11 medium to remove 98% of Pb, 88% of Cu, 82% of Cd, and 67% of Zn at  $5 \text{ mg L}^{-1}$  initial concentration of each metal. El-Sheekh et al. (2005) reported Mn removal by 32% and 100% from wastewater by cultures of *N. muscorum* and *Anabaena subcylindrica*, respectively, after 10 days of incubation. In the present

study, BA005 was more efficient in Mn removal compared to BA033 (Table 2). However, BA033 was more tolerant to Mn exposure, surviving in higher concentrations ( $>35 \text{ mg Mn L}^{-1}$ ). This difference can be attributed to the physiological characteristics of the species in dealing differently with the stress caused by Mn exposure. It has been reported that the presence of a structured envelope with abundant extracellular polymeric substances (EPS) can, at least partially, prevent the entry of Mn ions into cells (Mohamed 2001; Pereira et al. 2011). Further studies are clearly required to elucidate the role of EPS in the differential Mn tolerance observed here.

The concentration of Mn in the biomass washed with ultrapure water was significant, with high values of  $0.175 \text{ mg g}^{-1}$  for BA005 and  $0.139 \text{ mg g}^{-1}$  for BA033 (Fig. 6). However, after the biomass was washed with MES-EDTA, most of the Mn biosorbed was removed and any remaining amount was not detectable. This finding is consistent with the study of Keren et al. (2002), who demonstrated that most of the Mn biosorbed onto *Synechocystis* sp. is EDTA washable, which can penetrate the outer membrane of Gram-negative bacteria and remove Mn bound to this membrane. Together with EDTA chelating effect, it is possible that at pH 5.0 the  $\text{H}^+$  ions of the MES-EDTA buffer solution competed for the binding sites in the cyanobacterial cell wall, resulting in the removal of the biosorbed Mn. The surface structure of the cyanobacterial cell includes layers with unique functional molecular groups with diverse metal-binding capacity (Yee et al. 2004) that favor biosorption of Mn on the cell surface. The balance between the Mn fraction deposited in the cell outer membrane and that transported into the cell is dependent on specific trans-membrane transporters (Fischer et al. 2015; Brandenburg et al. 2017). The biosorption curves of the water-washed biomass from both species (Fig. 6) suggest that there was possibly saturation in BA005, however, testing biosorption at concentrations higher than  $35.4 \text{ mg Mn L}^{-1}$  is required to confirm this.

In the context of the potential for application in bioremediation approaches, both strains were tolerant to high concentrations of Mn relative to levels commonly found in contaminated water resources; these have been reported to range from  $0.01$  to  $10 \text{ mg L}^{-1}$  in natural waters such as lakes, streams, rivers, and oceans (Pinsino et al. 2012),  $0.5 \text{ mg L}^{-1}$  on average in drinking water originating from wells (Bouchard et al. 2007), and  $56 \text{ } \mu\text{g L}^{-1}$  to  $28.2 \text{ mg L}^{-1}$  in groundwater from a glacial aquifer system (Groschen et al. 2008).

### Ultrastructural effects of Mn exposure

To our knowledge this is the first study reporting the ultrastructural effects of Mn on the genera *Microcystis* and

*Nostoc* (Fig. 7). The increase in intrathylakoid spaces observed in cells exposed to Mn stress may be indicative of the ultrastructural plasticity of prokaryote cells as part of their adaptive adjustment. Brandenburg et al. (2017), using as model the cyanobacteria *Synechocystis* PCC 6803, identified a protein in the thylakoid membrane (Mnx) that functions as a thylakoid Mn transporter, proposed to export Mn from the cytoplasm to the thylakoid lumen, and helping maintain Mn homeostasis. The accumulation of Mn in the thylakoid in Mn enriched medium to alleviate cell damage is a hypothesis in agreement with our results of increased intrathylakoid spaces, although this requires further study. Reversible stretching and increase of the intrathylakoid space are adaptive aspects of configurational changes related to acclimatization to stress (Baulina 2012), as has been reported as a consequence of nutrient starvation (Hardie et al. 1983) and culture in dark (Gorelova and Baulina 2009). Furthermore, intrathylakoid spaces also indicate shutdown of the respiratory electron transport chain and the photosynthetic system in the membranes of thylakoids (Baulina 2012). Damage to the thylakoid membranes results in a decrease in photosynthetic activity and growth (Rangsayatorn et al. 2002), again in agreement with our data obtained from both species.

Carboxysomes are polyhedral bodies harboring the enzymes carbonic anhydrase (CA) and ribulose-1,5-bisphosphate carboxylase/oxygenase (Rubisco), responsible for CO<sub>2</sub> fixation and carboxylation in the Benson-Calvin cycle, respectively (Kupriyanova et al. 2013). The results obtained here indicated an increased number of carboxysomes in both species following exposure to increasing Mn concentrations, most likely due to high energetic requirements to overcome the toxic effects of Mn. Detail at the molecular level of the connections between growth and energetic requirements following Mn exposure in cyanobacterial strains still needs to be revealed in order to fully understand how they adjust their metabolism to support growth.

Polyphosphate granules (PP) are a primary source of phosphate. However, they also contain other ions such as magnesium, potassium and calcium (Andrade et al. 2004; Baulina 2012). It has been previously suggested that PP have an important role in the uptake of trace metals in cyanobacteria. The highly negatively charged lipids and proteins on the surface of PP act as an absorption site for the metal ions, contributing to cellular detoxification since the metal ions remain immobilized and unavailable within the granules (Jensen et al. 1982). Further studies have suggested a role of PP in cell detoxification under exposure to various metal ions in different groups of cyanobacteria. For instance, Rachlin et al. (1985) found an increase in PP after zinc exposure in *Anabaena flos-aquae* and *A. variabilis*, while Rangsayatorn et al. (2002) reported the same effect in

*Spirulina (Arthrospira) platensis* after exposure to cadmium. Similarly, Baxter and Jensen (1980) observed the presence of magnesium, strontium, barium and Mn in PP in cyanobacterial cells exposed to these metals. In accordance with several studies demonstrating that PP rapidly respond to environmental alterations, the increased number of PP observed in BA005 and BA033 illustrate a direct response to Mn that is likely to contribute to cellular detoxification.

## Conclusions

Our study demonstrated that cyanobacterial strains of different morphologies (BA005 and BA033) suffered acute toxicity due to Mn excess in culture media. Increasing Mn concentrations promoted physiological and morphological impairments in both strains, which were evidenced by a reduction in chlorophyll *a* content and growth rates coupled with ultrastructural changes including increased periplasmic space and intrathylakoid space, coupled with a higher number of carboxysomes and polyphosphate granules.

Although toxic effects were observed, the cyanobacterial strains investigated were tolerant to high concentrations of Mn relative to concentrations commonly reported in contaminated water resources. Both cyanobacterial strains examined here demonstrated potential for use in bioremediation of contaminated water. The strain BA005 showed greater potential at Mn concentrations lower than 30.0 mg L<sup>-1</sup>.

Few previous studies have addressed the toxicity of Mn in cyanobacteria and other aquatic organisms. Thus, the current study provides a foundation for measuring Mn toxicity in aquatic ecosystems, as well as improves our knowledge of the physiological and morphological responses of cyanobacteria following exposure to polluting concentrations of Mn. Although the precise mechanisms by which high levels of Mn interfere in cyanobacterial physiology remain to be elucidated, it is appropriate to expand the approach of the current study to a great number of cyanobacterial strains with different taxonomic affinities and origins.

**Acknowledgements** We thank Coordenação de Aperfeiçoamento de Pessoal de Nível Superior (CAPES) for the scholarship granted to KAFM, and the National Institute for Research and Technology on Mineral Resources, Water and Biodiversity—INCT-Acqua—for financial support. We acknowledge the Center of Microscopy of UFMG (<http://www.microscopia.ufmg.br>) for the TEM images and the Laboratory of Chemical Analysis of the Departamento de Engenharia Metalúrgica e de Materiais of the Engineering School/UFMG for the quantitative analysis of Mn. Funding from the Max Planck Society, the National Council for Scientific and Technological Development (CNPq-Brazil) and the Foundation for Research Assistance of the Minas Gerais State, Brazil (FAPEMIG, Grants APQ-01106-13 and APQ-01357-14) to WLA, and scholarships and a research fellowship

granted by CAPES/FAPEMIG (BPD-00514-14) and CAPES (PNPD-1638006) to MGMVV are gratefully acknowledged. PC is supported by NERC core funding to the British Antarctic Survey's 'Biodiversity, Evolution and Adaptation' Team.

## Compliance with ethical standards

**Conflict of interest** The authors declare that they have no conflict of interest.

**Publisher's note:** Springer Nature remains neutral with regard to jurisdictional claims in published maps and institutional affiliations.

## References

- Allen MM, Stanier RY (1968) Growth and division of some unicellular blue-green algae. *J Gen Microbiol* 51:199–202
- Andrade L, Keim CN, Farina M, Pfeiffer WC (2004) Zinc detoxification by a cyanobacterium from a metal contaminated bay in Brazil. *Braz Arch Biol Technol* 47:147–52
- Arunakumara KKIU, Xuecheng Z (2009) Effects of heavy metals (Pb<sup>2+</sup> and Cd<sup>2+</sup>) on the ultrastructure, growth and pigment contents of the unicellular cyanobacterium *Synechocystis* sp. PCC 6803\*. *Chin J Oceano Limn* 27:383–8
- Baulina OI (2012) Ultrastructural plasticity of cyanobacteria. Springer-Verlag, Berlin Heidelberg, London
- Baxter M, Jensen T (1980) Uptake of magnesium, strontium, barium, and manganese by *Plectonema boryanum* (Cyanophyceae) with special reference to polyphosphate bodies. *Protoplasma* 104:81–9
- Bender J, Gould JP, Vatcharapijarn Y, Young JS, Phillips P (1994) Removal of zinc and manganese from contaminated water with cyanobacteria mats. *Water Environ Res* 66:679–83
- Bonaventura C, Johnson FM (1997) Healthy environments for healthy people: bioremediation today and tomorrow. *Environ Health Persp* 105:5–20
- Bouchard M, Laforest F, Vandael L, Bellinger D, Mergler D (2007) Hair manganese and hyperactive behaviors: pilot study of school-age children exposed through tap water. *Environ Health Persp* 115:122–7
- Brandenburg F, Schoffman H, Kurz S, Krämer U, Keren N, Weber AP, Eisenhut M (2017) The *Synechocystis* manganese exporter Mnx is essential for manganese homeostasis in cyanobacteria. *Plant Physiol* 173:1798–810
- BRAZIL, Resolução CONAMA no. 357 (2005). Classificação de águas, doces, salobras e salinas do Território Nacional. Diário Oficial da União, 18 de março de 2005, seção 1, p. 58.
- Campos MMC, Faria VHF, Teodoro TS, Barbosa FA, Magalhães SM (2013) Evaluation of the capacity of the cyanobacterium *Microcystis novacekii* to remove atrazine from a culture medium. *J Environ Sci Heal B* 48:101–7
- Carrasco-Gil S, Rios JJ, Álvarez-Fernández A, Abadía A, García-Mina JM, Abadía J (2015) Effects of individual and combined metal foliar fertilisers on iron- and manganese-deficient *Solanum lycopersicum* plants. *Plant Soil* 402:27–45
- Chojnacka K, Noworyta A (2004) Evaluation of *Spirulina* sp. growth in photoautotrophic, heterotrophic and mixotrophic cultures. *Enzym Micro Tech* 34:461–5
- CICAD (2004) Manganese and its compounds: environmental aspects. Concise international chemical assessment document 63. WHO, Geneva, Switzerland, [http://www.who.int/ipcs/publications/cicad/cicad63\\_rev\\_1.pdf](http://www.who.int/ipcs/publications/cicad/cicad63_rev_1.pdf), Accessed 19 Sept 2018
- Csatorday K, Gombos Z, Szalontai B (1984) Mn<sup>2+</sup> and Co<sup>2+</sup> toxicity in chlorophyll biosynthesis. *P Natl Acad Sci* 81:476–8
- Dohnalkova A, Bilskis C, Kennedy D (2006) TEM study of manganese biosorption by Cyanobacterium *Synechocystis* 6803. *Microsc Micro* 12:444–5
- Duan N, Fan W, Changbo Z, Chunlei Z, Hongbing Y (2010) Analysis of pollution materials generated from electrolytic manganese industries in China. *Resour Conserv Recy* 54:506–11
- El-Sheekh MM, El-Shouny WA, Osman MEH, El-Gammal EWE (2005) Growth and heavy metals removal efficiency of *Nostoc muscorum* and *Anabaena subcylindrica* in sewage and industrial wastewater effluents. *Environ Toxicol Phar* 19:357–65
- Farag AM, Woodward DF, Goldstein JN, Brumbaugh W, Meyer JS (1998) Concentrations of metals associated with mining waste in sediments, biofilm, benthic macroinvertebrates, and fish from the Coeur d'Alene river basin, Idaho. *Arch Environ Con Tox* 34:119–27
- Fiore MF, Moon DH, Tsai SM, Lee H, Trevors JT (2000) Miniprep DNA isolation from unicellular and filamentous cyanobacteria. *J Microbiol Meth* 39:159–69
- Fischer WW, Hemp J, Johnson JE (2015) Manganese and the evolution of photosynthesis. *Orig Life Evol B* 45:351–7
- Frisbie SH, Mitchell EJ, Dustin H, Maynard DM, Sarkar B (2012) World health organization discontinues its drinking-water guideline for manganese. *Environ Health Perspect* 120:775–8
- Franco MW, Ferreira FAG, Vasconcelos IF, Batista BL, Pujoni DGF, Magalhães SMS, Barbosa Jr F, Barbosa FAR (2015) Arsenic biotransformation by cyanobacteria from mining areas: evidences from culture experiments. *Environ Sci Pollut R* 22:18607–15
- Genuário DB, Lorenzi AS, Agujaro LF, Isaac RL, Azevedo MTP, Neto RC, Fiore MF (2016) Cyanobacterial community and microcystin production in a recreational reservoir with constant *Microcystis* blooms. *Hydrobiologia* 779:105–25
- Genuário DB, Vaz MGMV, Hentschke GS, Sant'Anna CL, Fiore MF (2015) *Halotia* gen. nov., a phylogenetically and physiologically coherent cyanobacterial genus isolated from marine coastal environments. *Int J Syst Evol Micr* 65:663–75
- Genuário DB, Corrêa DM, Komárek J, Fiore MF (2013) Characterization of freshwater benthic biofilm-forming *Hydrocoryne* (Cyanobacteria) isolates from Antarctica. *J Phycol* 49:1142–53
- Gorelova OA, Baulina OI (2009) Ultrastructure of cyanobacterium *Nostoc* sp. f. *Blasia* cell forms in persisting populations. *Microbiology* 78:609–17
- Gorham PR, McLachlan J, Hammer U, Kim WK (1964) Isolation and culture of toxic strains of *Anabaena flos-aquae* (Lyng) de Breb. *Int Ver für Theor und Angew Limnol: Verh* 15:796–804
- Groschen GE, Arnold TL, Morrow WS, Warner KL (2008) Occurrence and distribution of iron, manganese, and selected trace elements in ground water in the glacial aquifer system of the Northern United States. *Sci Investig Rep* 2009–5006:89
- Hardie LP, Balkwill DL, Stevens SE (1983) Effects of iron starvation on the ultrastructure of the cyanobacterium *Agmenellum quadruplicatum*. *Appl Environ Microbiol* 45:1007–17
- Hazarika J, Pakshirajan K, Sinharoy A, Syiem MB (2014) Bioremoval of Cu(II), Zn(II), Pb(II) and Cd(II) by *Nostoc muscorum* isolated from a coal mining site. *J Appl Phycol* 27:1525–34
- Hrouzek P, Lukešová A, Mareš J, Ventura S (2013) Description of the cyanobacterial genus *Desmonostoc* gen. nov. including *D. muscorum* comb. nov. as a distinct, phylogenetically coherent taxon related to the genus *Nostoc*. *Fottea* 13:201–13
- Hudek L, Rai S, Michalczuk A, Rai LC, Neilan BA, Ackland ML (2012) Physiological metal uptake by *Nostoc punctiforme*. *Bio-metals* 25:893–903
- IGAM (2017) Instituto Mineiro de Gestão das águas. Encarte especial sobre a qualidade das águas do rio Doce após 2 anos do rompimento de barragem de Fundão 2015–2017, Belo Horizonte, Brazil, <http://www3.ana.gov.br/porta/ANA/sala-de-situacao/rio-doce/documentos-relacionados/encarte-qualidade-da-gua-do-rio>

- [doce-dois-anos-apos-rompimento-de-barragem-de-fundao-1.pdf](#), Accessed 19 Sept 2018
- Jensen TE, Baxter M, Rachlin JW, Jani V (1982) Uptake of heavy metals by plectonema into cellular components, especially polyphosphate bodies: an x-ray energy dispersive study. *Environ Pollut A* 27:119–27
- Ji L, Xie S, Feng J, Li Y, Chen L (2012) Heavy metal uptake capacities by the common freshwater green alga *Cladophora fracta*. *J Appl Phycol* 24:979–83
- Keren N, Kidd MJ, Penner-Hahn JE, Pakrasi HB (2002) A light-dependent mechanism for massive accumulation of manganese in the photosynthetic bacterium *Synechocystis* sp. PCC 6803. *Biochem-US* 41:15085–92
- Komárek J, Anagnostidis K (1989) Modern approach to the classification system of cyanophytes 4 –Nostocales. *Algological Studies*. 56:247–345
- Komárek J, Anagnostidis K (1998) Cyanoprokaryota 1. Teil: Chroococcales. Gustav Fischer Verlag Jena, Jena
- Komárek J, Anagnostidis K (2013) Cyanoprokaryota 3. Teil/ 3rd Part: Heterocytous Genera. Springer Spektrum, Berlin
- Komárek J, Kaštovský J, Mareš J, Johansen JR (2014) Taxonomic classification of cyanoprokaryotes (cyanobacterial genera) 2014, using a polyphasic approach. *Preslia* 86:295–335
- Komárek J (2016) Review of the cyanobacterial genera implying planktic species after recent taxonomic revisions according to polyphasic methods: state as of 2014. *Hydrobiologia* 764:259–70
- Kumar D, Rai J, Gaur JP (2012) Removal of metal ions by *Phormidium bigranulatum* (Cyanobacteria)-dominated mat in batch and continuous flow systems. *Bioresour Technol* 104:202–7
- Kupriyanova EV, Sinetova MA, Cho SM, Park YI, Los DA, Pronina NA (2013) CO<sub>2</sub>-concentrating mechanism in cyanobacterial photosynthesis: organization, physiological role, and evolutionary origin. *Photosynth Res* 117:133–46
- Lindon FC, Barreiro MG, Ramalho JC (2004) Manganese accumulation in rice: implications for photosynthetic functioning. *J Plant Physiol* 161:1235–44
- Lizieri C, Kuki KN, Aguiar R (2012) The morphophysiological responses of free-floating aquatic macrophytes to a supra-optimal supply of manganese. *Water Air Soil Poll* 223:2807–20
- Mateo P, Perona E, Berrendero E, Leganés F, Martín M, Golubic S (2011) Life cycle as a stable trait in the evaluation of diversity of *Nostoc* from biofilms in rivers. *FEMS Microbiol Ecol* 76:185–98
- Marschner H (1995) Mineral nutrition of higher plants, 2nd edn. Academic, London, p 889
- Meeks JC, Castenholz RW (1971) Growth and photosynthesis in an extreme thermophile *Synechococcus lividus*-I. Effect of temperature on fluorescence and enhancement of CO<sub>2</sub> assimilation. *J Therm Biol* 3:11–8
- Mohamed ZA (2001) Removal of cadmium and manganese by a non-toxic strain of the freshwater cyanobacterium *Gloeotheca magna*. *Water Res* 35:4405–9
- Neilan BA, Jacobs D, Del DT, Blackall LL, Hawkins PR, Cox PT, Goodman AE (1997) rRNA sequences and evolutionary relationships among toxic and nontoxic cyanobacteria of the genus *Microcystis*. *Int J Syst Evol Micr* 47:693–7
- OECD-The Organisation for Economic Co-operation and Development (2011) Test No. 201: Freshwater alga and cyanobacteria, growth inhibition test, OECD Guidelines for the Testing of Chemicals. OECD Publishing, Paris
- Pandey S, Rai R, Rai LC (2012) Proteomics combines morphological, physiological and biochemical attributes to unravel the survival strategy of *Anabaena* sp. PCC7120 under arsenic stress. *J Proteom* 75:921–37
- Papaefthimiou D, Hrouzek P, Mugnai MA, Lukesova A, Turicchia S, Rasmussen U, Ventura S (2008) Differential patterns of evolution and distribution of the symbiotic behaviour in Nostocacean cyanobacteria. *Int J Syst Evol Micr* 58:553–64
- Perales-Vela HV, Peña-Castro JM, Cañizares-Villanueva RO (2006) Heavy metal detoxification in eukaryotic microalgae. *Chemosphere* 64:1–10
- Pereira S, Micheletti E, Zille A, Santos A, Moradas-Ferreira P, Tamagnini P, Philippis R (2011) Using extracellular polymeric substances (EPS)-producing cyanobacteria for the bioremediation of heavy metals: do cations compete for the EPS functional groups and also accumulate inside the cell? *Microbiology* 157:451–58
- Pinsino A, Matranga V, Roccheri MC (2012) Manganese: a new emerging contaminant in the environment. In: Srivastava J (ed) Environmental contamination. In Tech Open Access Publisher, Rijeka, Croatia, pp. 17–36.
- Pokrovsky OS, Martinez RE, Golubev SV, Kompantseva EI, Shir-okova LS (2008) Adsorption of metals and protons on *Gloeocapsa* sp. cyanobacteria: A surface speciation approach. *Appl Geochem* 23:2574–88
- Rachlin JW, Jensen TE, Warkentine BE (1985) Morphometric analysis of the response of *Anabaena flos-aquae* and *Anabaena variabilis* (Cyanophyceae) to selected concentrations of zinc. *Arch Environ Con Tox* 402:395–402
- Rangsayatorn N, Upatham ES, Kruatrachue M, Pokethitiyooka P, Lanzac GR (2002) Phytoremediation potential of *Spirulina (Arthrospira) platensis*: Biosorption and toxicity studies of cadmium. *Environ Pollut* 119:45–53
- Reichman SM (2002) The responses of plants to metal toxicity: a review focusing on copper, manganese and zinc. Australian Minerals and Energy Environment Foundation, Melbourne, Australia, p 54
- Reynolds ES (1963) The use of lead citrate stain at high pH in electron microscopy. *J Cell Biol* 17:208–12
- Roy S (1997) Genetic diversity of manganese deposition in the terrestrial geological record. *Geol Soc Spec Publ* 119:5–27
- Siqueira MEPB (1985) Aspectos toxicológicos da exposição ao manganês. *Rev Bras Saude Ocup* 13:28–36
- Spurr AR (1969) A low-viscosity epoxy resin embedding medium for electron microscopy. *J Ultra Mol Struct R* 26:31–43
- Tamura K, Peterson D, Peterson N, Stecher G, Nei M, Kumar S (2011) MEGA5: molecular evolutionary genetics analysis using maximum likelihood, evolutionary distance, and maximum parsimony methods. *Mol Biol Evol* 28:2731–9
- Taton A, Grubisic S, Brambilla E, Wit RD, Wilmotte A (2003) Cyanobacterial diversity in natural and artificial microbial mats of Lake Fryxell (McMurdo Dry Valleys, Antarctica): a morphological and molecular approach. *Appl Environ Micro* 69:5157–69
- Teixeira IR, Borém A, Andrade MJB, Giúdice MPD, Cecon PR (2004) Chlorophyll levels in common bean plants as influence by manganese and zinc fertilization. *Acta Sci Agron* 26:147–52
- Truus K, Viitak A, Vaher M, Muinasmaa U, Paasrand K, Tuvikene R, Levandi T (2007) Comparative determination of microelements in Baltic seawater and brown algae samples by atomic absorption spectrometric and inductively coupled plasma methods. *Proc Estonian Acad Sci Chem* 56:122–33
- Vaz MGMV, Genuário DB, Andreote APD, Malone CFS, Sant'Anna CL, Barbiero L, Fiore MF (2015) *Pantalaninema* gen. nov. and *Alkalinema* gen. nov.: novel Pseudanabaenacean genera (Cyanobacteria) isolated from saline-alkaline lakes. *Int J Syst Evol Micr* 65:298–308
- Vidali M (2001) Bioremediation. An overview. *Pure Appl Chem* 73:1163–72
- Yee N, Benning LG, Phoenix VR, Ferris FG (2004) Characterization of metal-cyanobacteria sorption reactions: a combined macroscopic and infrared spectroscopic investigation. *Envir Sci Tech Lib* 38:775–82